Multiphase reactivity of polycyclic aromatic hydrocarbons is driven by phase separation and diffusion limitations

Shouming Zhou[a,1], Brian C. H. Hwang[b,1], Pascale S. J. Lakey[b], Andreas Zuend[c], Jonathan P. D. Abbatt[a,2], and Manabu Shiraiwa[b,2]

[a]Department of Chemistry, University of Toronto, Toronto, M5S 3H6, Canada; [b]Department of Chemistry, University of California, Irvine, CA 92697; and [c]Department of Atmospheric and Oceanic Sciences, McGill University, Montreal, H3A 0B9, Canada

Benzo[a]pyrene (BaP), a key polycyclic aromatic hydrocarbon (PAH) often associated with soot particles coated by organic compounds, is a known carcinogen and mutagen. When mixed with organics, the kinetics and mechanisms of chemical transformations of BaP by ozone in indoor and outdoor environments are still not fully elucidated. Using direct analysis in real-time mass spectrometry (DART-MS), kinetics studies of the ozonolysis of BaP in thin films exhibited fast initial loss of BaP followed by a slower decay at long exposure times. Kinetic multilayer modeling demonstrates that the slow decay of BaP over long times can be simulated if there is slow diffusion of BaP from the film interior to the surface, resolving long-standing unresolved observations of incomplete PAH decay upon prolonged ozone exposure. Phase separation drives the slow diffusion time scales in multicomponent systems. Specifically, thermodynamic modeling predicts that BaP phase separates from secondary organic aerosol material so that the BaP-rich layer at the surface shields the inner BaP from ozone. Also, BaP is miscible with organic oils such as squalane, linoleic acid, and cooking oil, but its oxidation products are virtually immiscible, resulting in the formation of a viscous surface crust that hinders diffusion of BaP from the film interior to the surface. These findings imply that phase separation and slow diffusion significantly prolong the chemical lifetime of PAHs, affecting long-range transport of PAHs in the atmosphere and their fates in indoor environments.

phase state | ozone | indoor chemistry | bulk diffusion | kinetic modeling

Polycyclic aromatic hydrocarbons (PAHs), including benzo[a] pyrene (BaP), are among the most prominent toxic air pollutants, posing a threat to human health because their metabolites and oxidation products are carcinogenic and mutagenic (1). PAHs are emitted into the atmosphere from incomplete combustion and biomass burning and by smoking and cooking in indoor environments. Due to its low vapor pressure, BaP resides mostly in the condensed phase, and heterogeneous oxidation of BaP by oxidants such as OH and O_3 is a major atmospheric loss pathway (2). Laboratory measurements show rapid degradation of BaP against ozone when adsorbed to a variety of substrates such as water, ammonium sulfate, soot, and organic compounds (3–6).

Upon chemical aging in the atmosphere, PAH-containing particles are likely coated by semi- or low-volatile organic compounds, which are formed by multigenerational gas-phase oxidation of volatile organic compounds. Laboratory experiments have shown that organic coatings can retard multiphase reactions of ozone with PAHs due to kinetic limitations of bulk diffusion (3, 7, 8). The extent of coating effects depends on the phase state of organic coatings, which can be liquid, amorphous semisolid, or glassy solid, depending on chemical composition, relative humidity (RH), and temperature (9). This shielding effect of PAHs from oxidation was recently implemented into regional and global air-quality models showing how regional and global distributions and

transport of BaP can be affected by the temperature and humidity dependence of diffusivity and reactivity of BaP-containing particles (10, 11). These modeling results are consistent with observations of BaP at remote terrestrial and marine sites, even in the polar regions (2, 12).

Atmospheric aerosol particles are often mixtures of organics, inorganics, and water, which are subject to complex and nonideal behavior including liquid–liquid and/or liquid–solid phase separation, as predicted by thermodynamic models (13, 14). Experimental studies have demonstrated the existence of multiple phases in model mixtures or laboratory-generated secondary organic aerosol (SOA) particles as well as in field-collected organic aerosol particles (15–17). Liquid–liquid phase separation was also observed in SOA particles free of inorganic salts (18–20). The interplay of phase state and nonideality can affect aerosol mass concentration and the characteristic time scale of gas-particle mass transfer (21). Changes in viscosity upon chemical aging of organic particles were observed (22), but it is not yet clear how the effects and interplay of nonideality and phase state evolve upon multiphase chemical interactions to affect fates and atmospheric long-range transport of organic compounds.

Significance

Polycyclic aromatic hydrocarbons (PAHs) are among the most prominent toxic compounds in the air. Heterogeneous reactions involving O_3 can change the toxicity of PAHs, but the reaction mechanism and kinetics remain to be elucidated. Based on new experiments combined with state-of-the-art kinetic and thermodynamic models, we show that phase separation plays a critical role in the ozonolysis of PAHs mixed with secondary organic aerosols and organic oils. Ozonolysis products of PAHs phase separate to form viscous surface crusts, which protect underlying PAHs from ozonolysis to prolong their chemical lifetime. These results have significant implications for outdoor and indoor air quality by affecting PAH long-range transport and fate in indoor environments.

Although extensive laboratory measurements and modeling of PAHs have been conducted under atmospherically relevant conditions, chemical transformation of PAHs in indoor environments, where we spend ~90% of the time, is poorly understood (23). PAHs can be transported from outside air and can also be emitted by indoor activities such as smoking, cooking, and burning of solid fuels (24). Recent findings show that BaP diol-epoxide products, which are highly carcinogenic, can be formed in indoor environments (25), and chronic exposure to these compounds can be detrimental to human health. Thus, both the chemical transformation of PAHs with gaseous ozone under indoor-relevant conditions and the PAH reactivity in mixtures of chemicals emitted from indoor sources need to be elucidated. A long-standing, unexplained issue in the field of environmental chemistry and health is the observation that although ozonolysis experiments show a rapid initial loss of condensed-phase PAHs, prolonged exposure to ozone does not necessarily lead to complete PAH decay (26–29).

In this study, the decay kinetics of BaP upon exposure to ozone were measured using direct analysis in real-time mass spectrometry (DART-MS). Three different sets of experimental and modeling scenarios were explored: (*i*) the ozonolysis kinetics of pure BaP films (containing a small amount of an internal standard); (*ii*) the effects of the reaction substrate by mixing BaP with α-pinene SOA material, a mixture of different oxidized organic compounds; and (*iii*) the effects of mixing BaP with liquid substrates such as squalane, linoleic acid, and cooking oil. The experimental conditions were simulated using the kinetic multilayer model of aerosol surface and bulk chemistry (KM-SUB), which resolves mass transport and chemical reactions at the surface and in the condensed phase explicitly (30), combined with the Aerosol Inorganic-Organic Mixtures Functional Groups Activity Coefficients (AIOMFAC) thermodynamic model (31–33) at the core of a thermodynamic equilibrium framework that predicts chemical composition of different coexisting phases. Together, the 3 sets of simulations and experimental results pinpoint the critical factors that control PAH ozonolysis loss rates in a variety of organic media.

Results and Discussion

Fig. 1 shows the ozonolysis decays of pure BaP in thin films that only contain traces of bis(2-ethylhexyl) sebacate (BES) as an internal standard. There is a 1-h exposure to 15 to 1,000 ppb ozone (O_3) at <5% RH and 296 K. If the BaP were uniformly deposited on the capillary, then the resulting film would be roughly 1 monolayer thick. Much more likely, the film has inhomogeneous thickness, leading to most of the BaP being present in multilayer amounts. The BaP concentration decayed slower at 15 ppb O_3 than at 100 ppb O_3, while BaP decay rates became saturated and very similar at 500 and 1,000 ppb O_3. Interestingly, BaP was not entirely reacted away, leaving an unreacted fraction of ~20% at high O_3 mixing ratios (500 and 1000 ppb) after 1 h, which has also been observed previously, but not explained for many decades (26–29). KM-SUB was applied to simulate these data by considering surface adsorption of O_3, decomposition of O_3 into reactive oxygen intermediates (ROIs; e.g., sorbed O atoms) and subsequent reactions with BaP (34), bulk diffusion of O_3 and BaP, and bulk reactions between O_3 and BaP. The time and concentration dependence of BaP decay can be reproduced by KM-SUB with the kinetic parameter values listed in *SI Appendix*, Table S1, as consistent with our previous work (34). The film thickness was set in the model to be 0.61 nm, representing roughly a double layer of molecules. Note that qualitatively similar modeling results were obtained using a film thickness 10 times larger (see *SI Appendix* for details).

The modeling results indicate that the decay of BaP is initially controlled by ROI formation and surface reactions with BaP, leading to fast initial BaP decay. Once surface BaP is depleted,
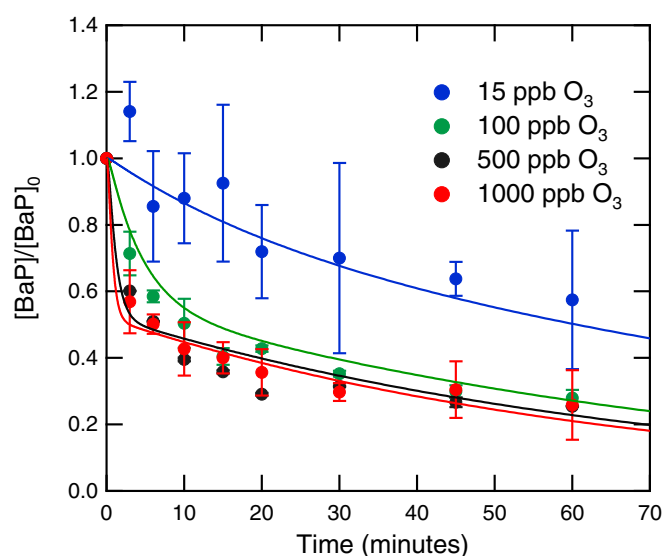

Fig. 1. Decay of BaP concentration in BaP/BES films exposed to different mixing ratios of ozone (15 to 1,000 ppb) at 296 K and RH <5%. Filled circles show the experimental data, with error bars representing the SD of 10 measurements. The solid lines are KM-SUB simulation results with a single kinetic parameter set shown in *SI Appendix*, Table S1.

the key aspect of the model prediction is that the oxidation of BaP becomes limited by bulk diffusion of BaP from the film interior to the surface at longer reaction times. This explains the subsequent slow BaP decay after ~10 min, as well as the saturation of BaP decay rates at higher O_3 mixing ratios. Bulk diffusivity of BaP was predicted to be in the range of ~10^{-17} to 10^{-19} cm^2·s^{-1}, which is consistent with an amorphous semisolid state of the film. Note that the modeled kinetics are insensitive to the bulk diffusivity of O_3, as bulk reactions play a minor role in overall BaP degradation (3, 7). As a consequence, BaP in the deep bulk is protected from ozonolysis due to this shielding effect arising from slow BaP diffusion to the surface, which explains the unreacted BaP fraction at long reaction times in these and previous experiments (26–29).

The results from the second reaction scenario are shown in Fig. 2*A*, which illustrates the time-dependent oxidative decay of BaP mixed with α-pinene SOA exposed to 500 ppb O_3 at dry conditions, 50% RH, and 85% RH. The BaP concentration decays at very similar rates at different RHs for up to ~10 min and then decays with faster rates and higher reacted fractions at higher RH. In theory, this behavior could be due to a phase change of α-pinene SOA, which is expected to exist as an amorphous solid at a temperature of ~295 K and at dry conditions but becomes substantially less viscous at higher RH due to water uptake (35). According to previous viscosity measurements (35) and kinetics experiments (7), the bulk diffusivity of PAH in α-pinene SOA at 85% RH is expected to be as high as ~10^{-11} cm^2·s^{-1}. However, when PAH is assumed to be well mixed and with such a high bulk diffusivity in the α-pinene SOA mixture, the KM-SUB simulation failed to reproduce the experimental data, as shown by the red dashed line in Fig. 2*A*. Under such assumptions, KM-SUB predicts complete depletion of BaP within 1 h, indicating a lack of substantial kinetic limitations, even at 85% RH. There is clearly an aspect to this modeling scenario that is not accurately representing the experimentally observed kinetics.

To probe this reaction system more deeply, the likelihood of phase separation was assessed using the AIOMFAC-based liquid–liquid equilibrium (LLE) model (31–33), where α-pinene SOA was simulated by a mixture of 14 representative oxidation products (*SI Appendix*, Table S2) (13, 21). Contrary to the assumption of full
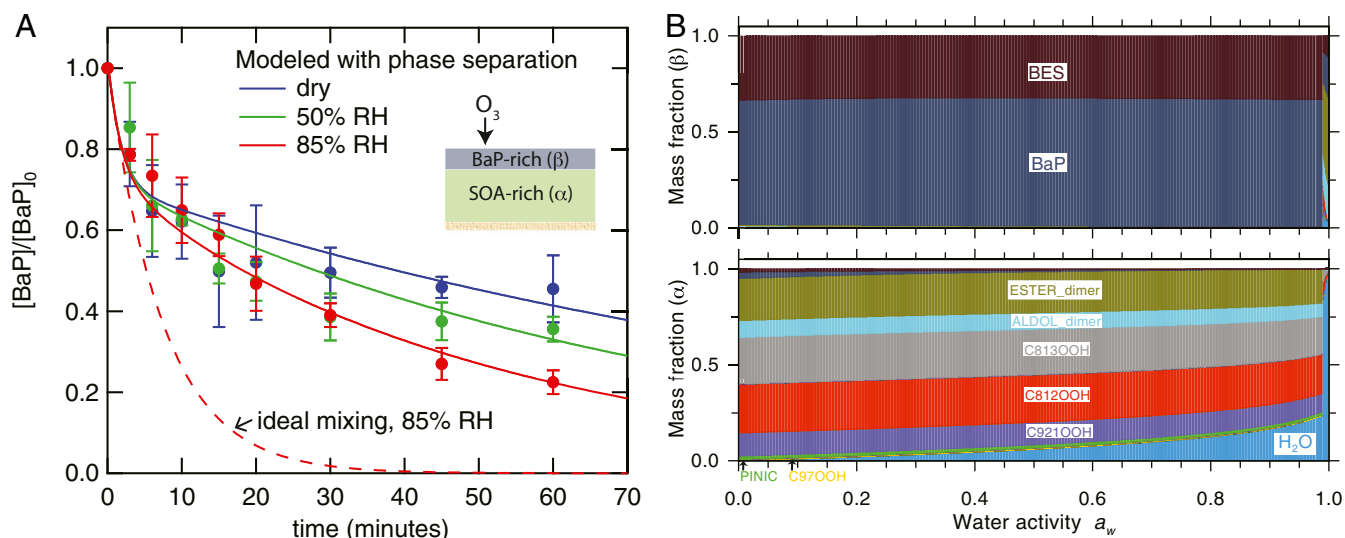
Fig. 2. (*A*) Decay of BaP embedded in the films of α-pinene SOA upon exposure to 500 ppb O₃ at dry conditions (blue), 50% RH (green), and 85% RH (red) at 296 K. The circle markers are the experimental data, and error bars represent the SD of 10 measurements. KM-SUB modeling results are presented with consideration of liquid–liquid phase separation (solid lines) and without (dashed line for 85% RH). (*B*) Thermodynamic modeling results by AIOMFAC predicting phase compositions of the α-pinene SOA + BaP/BES system as a function of water activity (i.e., RH) for an initial amount of 10 ng of α-pinene SOA, 1 ng of BaP, and 0.5 ng of BES in the particle phase; i.e., before reaction with ozone. In particular, each frame corresponds to a different phase, within which the relative proportions of different components in the phase are indicated. Specifically, predicted phase compositions are shown as stacked mass fractions of the individual components for the phase α enriched by SOA compounds (*Lower*) and the phase β dominated by BaP and BES (*Upper*). Note that α-pinene SOA is treated as comprising 14 representative oxidation products (see *SI Appendix,* Table S3 for explanation of labels).

mixing which led to the dashed line in Fig. 2*A*, the LLE model predicts that the mixtures separate into BaP-rich (Fig. 2 *B*, *Upper*) and SOA-rich (Fig. 2 *B*, *Lower*) phases of distinct compositions, dependent on the water activity. Under dry conditions, ∼65% of the total particle-bound BaP mass is predicted to partition to the phase rich in BES and BaP, with the remaining ∼35% BaP present in the SOA-rich phase. BaP's phase preference becomes more distinct with increasing RH so that at 50% RH, about 90% of its mass resides in the BaP-rich phase, and at 85% RH, the partitioning to the BaP-rich phase approaches 100%; that is, virtually complete phase separation. The BaP-rich phase is most likely in the form of a film on top of the SOA-rich phase (i.e., full engulfing as opposed to partial engulfing), considering that BaP should have lower surface tension than polar SOA materials.

By implementing the predicted phase compositions arising from phase separation in KM-SUB, the model reproduces experimental data very well, as shown by the solid lines in Fig. 2*A*. The kinetic model simulations reveal that the BaP decay is initially controlled by surface reactions leading to fast BaP decay, followed by diffusion of BaP molecules from the bulk to its surface. The diffusion coefficients of BaP within the surface crust (i.e., a semisolid surface layer of high viscosity) were found to have the most sensitivity in the modeling. Reactions at the surface are found to be faster than in the bulk (7), so BaP in the film interior needs to diffuse through the bulk to the surface to react. The BaP-rich layer at the surface hinders the BaP in the film interior to diffuse to the surface, resulting in significant fractions of BaP remaining unreacted after 1 h of ozone exposure.

The final set of kinetics experiments measured the decay behavior of BaP embedded in other organic liquids, including squalane, linoleic acid, and cooking oil, as shown in Fig. 3. Contrary to the SOA case, BaP is miscible with these organic compounds, as evident by visual inspection and as predicted by the thermodynamic phase equilibrium model. So, BaP should initially be homogenously mixed within the film. The KM-SUB modeling results for BaP decay in squalane upon exposure to 500 ppb O₃ are shown as the dashed red line in Fig. 3. The model

captures the initial BaP decay up to ∼10 min but overpredicts the long-term BaP decay in the absence of kinetic limitations.

Although BaP may be miscible initially, its oxidation products may phase separate from the oily liquid reaction substrates. We considered 3 major BaP ozonolysis products, including 6,12-dihydroxy-BaP, BaP-6,12-dione, and a BaP-derived dicarboxylic acid (36), and cooking oil was treated as triolein (*SI Appendix,* Table S3). The AIOMFAC thermodynamic equilibrium modeling revealed that these oxidation products are immiscible with all 3 organic liquids and the system should therefore undergo phase separation upon formation of such oxidation products (Fig. 3*B* and *SI Appendix,* Fig. S1). This suggests that the oxidation process, which leads to the formation of oxidation products that are more oxygenated than the BaP reactant, promotes phase separation. A viscous surface crust forms, which can hinder diffusion of BaP from the film interior to the surface. We note that a crusting effect has been observed in the uptake of organic nitrates (37) or ammonia to SOA, where carboxylates may also form a viscous crust at the surface of the reaction substrate (38).

To consider this effect in KM-SUB, bulk diffusion coefficients of BaP were treated as composition dependent using the Vignes-type equation (39) (*SI Appendix,* Fig. S2). Linoleic acid, and cooking oil compounds are unsaturated (i.e., with C=C double bonds), and ozone reacts with these compounds (*SI Appendix,* Fig. S3). Previous studies have shown that high-molar-mass compounds such as peroxidic oligomers can be formed, especially under low RH (40, 41), causing an increase of viscosity (22). Thus, these products may also contribute to form the surface crust, which was explicitly treated in KM-SUB. With consideration of these effects, KM-SUB was able to capture a slow BaP decay at longer reaction times to fully reproduce the experimental data, as shown by the solid lines in Fig. 3. Retardation of oleic acid ozonolysis from surface crust formation has been observed in mixed-component particles in previous studies (42–44). These results demonstrate how phase separation leading to crust formation at the surface can affect the chemical transformation of PAH in multicomponent mixtures.
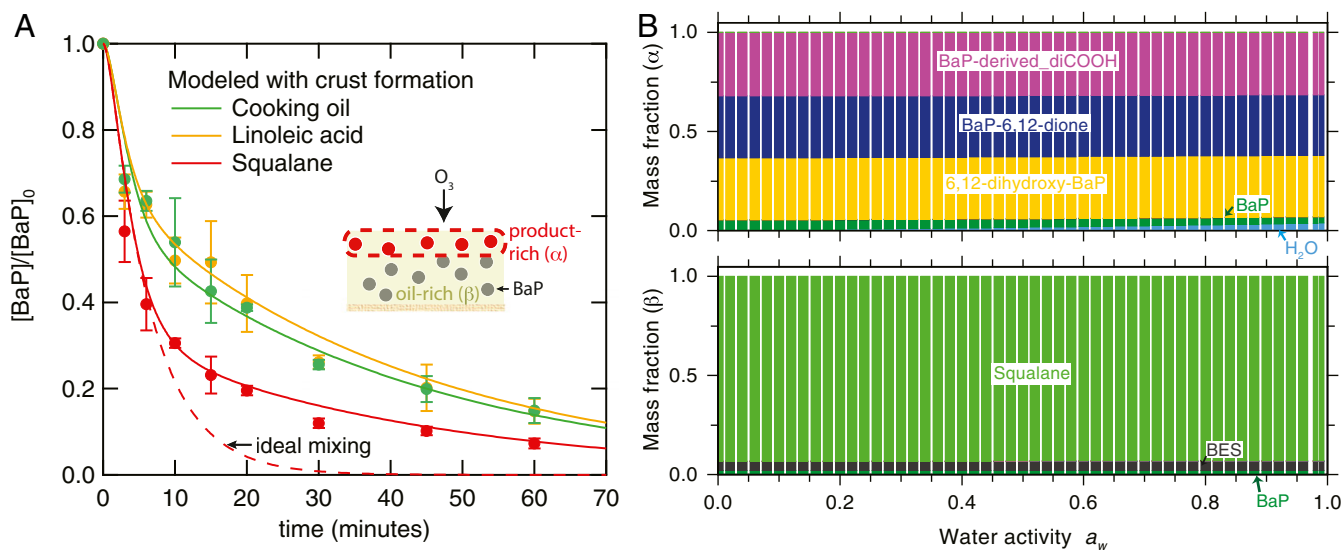
Fig. 3. (A) Decay of BaP embedded in the films of squalane (red), linoleic acid (yellow), or cooking oil (green) upon exposure to 500 ppb O_3 under dry conditions. The circle markers are the experimental data, and error bars represent the SD of 10 measurements. The solid lines represent KM-SUB simulations with consideration of surface crust formation by BaP oxidation products and composition-dependent bulk diffusivity using a Vignes-type equation, while the dashed line for the squalane case does not consider this phase separation effect, failing to reproduce experiments. (B) Predicted phase compositions in mass fractions for mixtures of BaP, BaP oxidation products (BaP-6,2-dione, BaP-derived carboxylic acid, and 6,12-dihydroxy BaP), and squalane after half of the BaP is degraded (see Fig. 2B caption for explanation of the plots). One phase consists largely of squalane, BES, and BaP (β, *Lower*), whereas the other consists largely of the BaP oxidation products (α, *Upper*). LLE calculations with AIOMFAC predict for all RH (or water activities) that BaP oxidation products are virtually immiscible in squalane.

Implications for Atmospheric and Indoor Chemistry. PAHs are often associated with soot particles that are subject to coating by semivolatile primary organic emissions and by secondary organic materials formed by oxidation of anthropogenic and biogenic precursors. Our experimental and modeling study demonstrates that the multiphase reactivity of PAHs depends strongly on the interplay of phase state and nonideal mixing with such organic materials.

In all 3 sets of reaction systems, it was found that slow diffusion through viscous phases is rate limiting at long reaction times because the BaP must diffuse to the surface to react. In the case of pure BaP films, the semisolid substrate acts as the diffusion barrier, whereas in the mixtures with oils such as squalane, linoleic, or cooking oils, the reaction products phase separate into a phase with low diffusivity. When mixed into SOA, the PAHs do not mix homogeneously with α-pinene SOA but are instead separated into different phases, affecting the multiphase reactivity of PAHs against ozone. RH controls the degree of nonideality and phase separation and also determines the phase state of PAH–SOA mixtures. In phase-separated particles with the PAH-rich phase on the particle surface, slow diffusion of PAH from the particle bulk to the surface limits PAH degradation by ozone. Moreover, the SOA-rich phase, which embeds a fraction of the PAHs, adopts an amorphous (semi)solid state at low RH, posing additional kinetic limitations of bulk diffusion and retarding ozonolysis kinetics. Overall, these effects will prolong chemical lifetimes of PAHs, facilitating long-range transport of PAHs and affecting regional and global distributions in the atmosphere and their effects on air quality and public health (10, 11).

PAHs are also found in indoor environments, and a BaP concentration of 38.8 μg/g of dust has been reported (45). PAHs are transported from outdoors to indoors and are directly emitted by indoor activities such as cooking and smoking. With cooking, BaP may be deposited and embedded into an organic film on indoor surfaces. The fate of low-volatility PAHs will be controlled by surface oxidative processes, considering the high surface-to-volume ratios in indoor environments and that

organic films can persist for an indefinite time unless they are wiped off (46).

To investigate PAH degradation kinetics with real indoor air, a BaP film was exposed to room air containing 10 ppb O_3 for up to 5 h. The BaP decay rate by room air is remarkably similar to the one when BaP is exposed to 15 ppb O_3 in a controlled flow tube setting, and it is modeled well (the solid red line in *SI Appendix*, Fig. S4) with the same kinetic parameters used to model Fig. 1. These results indicate that ozone will be the most
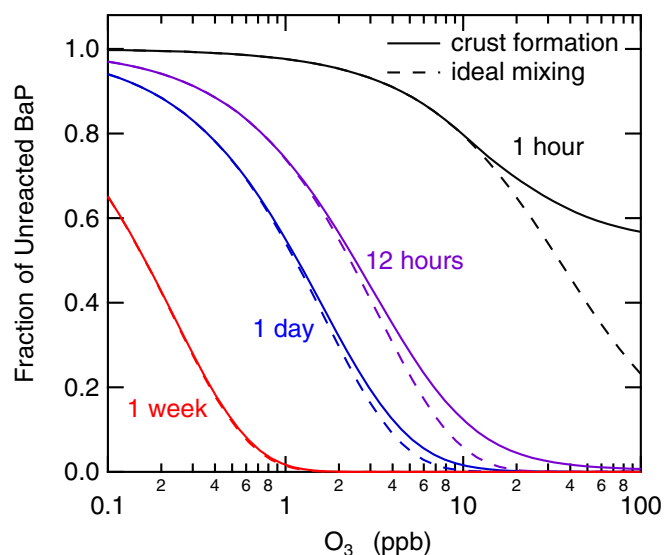

Fig. 4. Fraction of BaP remaining in an 8-nm-thick cooking oil film exposed to different gas-phase ozone mixing ratios after 1 h (black), 12 h (purple), 1 d (blue), and 1 wk (red) at 295 K and dry conditions, as simulated by KM-SUB considering phase separation and crust formation by BaP oxidation products (solid lines) or assuming ideal mixing (dashed lines).

important indoor oxidant, among others (e.g., OH, NO$_3$), for determining the fate of these compounds in indoor environments.

To illustrate the chemical fate of BaP embedded in an indoor surface film consisting of cooking oil, we simulated the molar fraction of unreacted BaP after exposure to 0.1 to 100 ppb O$_3$ for 1 h, 12 h, 1 d, and 1 wk. The parameters used in the model are those that successfully modeled the experimental data in Fig. 3 (*SI Appendix*, Table S1). The mass concentration of BaP in cooking oil was assumed to be 1,200 ng·cm^{-3} and the film thickness was set to be 8 nm based on previous observations in indoor environments (47–49). Fig. 4 shows the results of such KM-SUB simulations. At an O$_3$ concentration of 10 ppb, ~80% and ~10% of the BaP remain unreacted after 1 h and 12 h, respectively, whereas the BaP is expected to be fully reacted away after 1 wk. Typical indoor O$_3$ concentrations range from 5 ppb to over 50 ppb (depending on air exchange rates and outdoor air pollution) (50), and the unreacted fraction of BaP molecules considering surface crust formation is larger than the case with an ideal mixing assumption, especially at higher O$_3$ concentrations. Thus, the fate of PAH in indoor environments is strongly influenced by multiphase reactivity as impacted by surface crust formation and diffusion limitations. The true BaP lifetime may be even longer and is dependent upon the mass transfer rates that prevail under genuine indoor conditions.

Materials and Methods

Kinetics Experiments. A solution containing BaP and BES was deposited on the outside sealed end of glass melting point capillary tubes, and a thin film of BaP/BES was formed after the solvent evaporated. BaP was also mixed with other organics, namely squalane, cooking oil, linoleic acid, or SOA, as formed in a 1-m^3 Teflon chamber from the dark reaction of α-pinene with ozone. Heterogeneous oxidation of BaP with ozone was carried out at 295 ± 3 K in a flow tube. The indoor air oxidation of BaP was performed by placing the capillaries inside a fume hood in the Chemistry Department, University of Toronto, where the temperature, RH, and ozone mixing ratio was monitored. After oxidation, the capillaries were stored in a desiccator where a flow of nitrogen was added to avoid contamination/oxidation from the room air before analysis using DART-MS, with the approach described in full previously (51). Further details are described in *SI Appendix*.

Kinetic and Thermodynamic Modeling. KM-SUB (30) was used for simulating kinetics experiments of BaP ozonolysis. The AIOMFAC thermodynamic model (31–33) was used to estimate thermodynamic mixing and the potential for phase separation in the PAH/organics/water system. Predicted phase compositions and associated-component activity coefficients were considered in KM-SUB. KM-SUB consists of a number of compartments and layers in which ozone, BaP, and oxidized products can undergo mass transport and chemical reactions in the particle phase. Decomposition of surface-adsorbed ozone into ROIs (e.g., O atoms) followed by surface reactions with BaP was simulated explicitly. The required kinetic parameters include the surface accommodation coefficient and the desorption lifetime of ozone, bulk diffusion coefficients of ozone and BaP, and the second-order surface and bulk reaction rate coefficients between ozone and BaP as well as those between ozone and unsaturated organic oils (*SI Appendix*, Table S1). Nanoscale effects are not considered in this modeling. While beyond the scope of this study, they would need to be included to more accurately describe the composition and behavior of very thin surface layers. From theoretical considerations and experimental work, it is known that the influence of liquid–liquid and air–liquid interfaces becomes increasingly important at the nanometer scale (52, 53). The proximity of molecules/phases to such interfaces can lead to enhancement or reduction of the thermodynamic drivers for phase separation and/or bulk–surface partitioning, depending on the system (54, 55). Hence, the AIOMFAC-based calculations, while performed for bulk-system conditions, also apply approximately to nanoscale systems for the case where the interfacial energy effects nearly balance. The degree to which this case applies to the systems studied here is unknown yet is of interest for future experimental and modeling studies on aerosol size and interface effects. Further method details are described in *SI Appendix*.

1. B. J. Finlayson-Pitts, J. N. Pitts, Jr, Tropospheric air pollution: Ozone, airborne toxics, polycyclic aromatic hydrocarbons, and particles. *Science* **276**, 1045–1052 (1997).
2. I. J. Keyte, R. M. Harrison, G. Lammel, Chemical reactivity and long-range transport potential of polycyclic aromatic hydrocarbons–A review. *Chem. Soc. Rev.* **42**, 9333–9391 (2013).
3. S. Zhou, A. K. Y. Lee, R. D. McWhinney, J. P. D. Abbatt, Burial effects of organic coatings on the heterogeneous reactivity of particle-borne benzo[a]pyrene (BaP) toward ozone. *J. Phys. Chem. A* **116**, 7050–7056 (2012).
4. N. O. A. Kwamena, M. G. Staikova, D. J. Donaldson, I. J. George, J. P. D. Abbatt, Role of the aerosol substrate in the heterogeneous ozonation reactions of surface-bound PAHs. *J. Phys. Chem. A* **111**, 11050–11058 (2007).
5. B. T. Mmereki, D. J. Donaldson, Direct observation of the kinetics of an atmospherically important reaction at the air-aqueous interface. *J. Phys. Chem. A* **107**, 11038–11042 (2003).
6. U. Pöschl, T. Letzel, C. Schauer, R. Niessner, Interaction of ozone and water vapor with spark discharge soot aerosol particles coated with benzo[a]pyrene: O$_3$ and H$_2$O adsorption, benzo[a]pyrene degradation, and atmospheric implications. *J. Phys. Chem. A* **105**, 4029–4041 (2001).
7. S. Zhou, M. Shiraiwa, R. D. McWhinney, U. Pöschl, J. P. D. Abbatt, Kinetic limitations in gas-particle reactions arising from slow diffusion in secondary organic aerosol. *Faraday Discuss* **165**, 391–406 (2013).
8. E. A. Henderson, D. J. Donaldson, Influence of organic coatings on pyrene ozonolysis at the air-aqueous interface. *J. Phys. Chem. A* **116**, 423–429 (2012).
9. M. Shiraiwa et al., Global distribution of particle phase state in atmospheric secondary organic aerosols. *Nat. Commun.* **8**, 15002 (2017).
10. Mu Q et al., Temperature effect on phase state and reactivity controls atmospheric multiphase chemistry and transport of PAHs. *Sci. Adv.* **4**, eaap7314 (2018).
11. M. Shrivastava et al., Global long-range transport and lung cancer risk from polycyclic aromatic hydrocarbons shielded by coatings of organic aerosol. *Proc. Natl. Acad. Sci. U.S.A.* **114**, 1246–1251 (2017). Erratum in: *Proc. Natl. Acad. Sci. U.S.A.* **114**, E2263 (2017).
12. C. J. Halsall et al., Spatial and temporal variation of polycyclic aromatic hydrocarbons in the Arctic atmosphere. *Environ. Sci. Technol.* **31**, 3593–3599 (1997).
13. A. Zuend, J. H. Seinfeld, Modeling the gas-particle partitioning of secondary organic aerosol: The importance of liquid-liquid phase separation. *Atmos. Chem. Phys.* **12**, 3857–3882 (2012).
14. E. I. Chang, J. F. Pankow, Prediction of activity coefficients in liquid aerosol particles containing organic compounds, dissolved inorganic salts, and water–Part 2: Consideration of phase separation effects by an X-UNIFAC model. *Atmos. Environ.* **40**, 6422–6436 (2006).
15. C. Pöhlker et al., Biogenic potassium salt particles as seeds for secondary organic aerosol in the Amazon. *Science* **337**, 1075–1078 (2012).
16. Y. You et al., Images reveal that atmospheric particles can undergo liquid-liquid phase separations. *Proc. Natl. Acad. Sci. U.S.A.* **109**, 13188–13193 (2012).
17. U. K. Krieger, C. Marcolli, J. P. Reid, Exploring the complexity of aerosol particle properties and processes using single particle techniques. *Chem. Soc. Rev.* **41**, 6631–6662 (2012).
18. M. Song, S. Ham, R. J. Andrews, Y. You, A. K. Bertram, Liquid–liquid phase separation in organic particles containing one and two organic species: Importance of the average O:C. *Atmos. Chem. Phys.* **18**, 12075–12084 (2018).
19. M. Song, P. Liu, S. T. Martin, A. K. Bertram, Liquid–liquid phase separation in particles containing secondary organic material free of inorganic salts. *Atmos. Chem. Phys.* **17**, 11261–11271 (2017).
20. L. Renbaum-Wolff et al., Observations and implications of liquid–liquid phase separation at high relative humidities in secondary organic material produced by α-pinene ozonolysis without inorganic salts. *Atmos. Chem. Phys.* **16**, 7969–7979 (2016).
21. M. Shiraiwa, A. Zuend, A. K. Bertram, J. H. Seinfeld, Gas-particle partitioning of atmospheric aerosols: Interplay of physical state, non-ideal mixing and morphology. *Phys. Chem. Chem. Phys.* **15**, 11441–11453 (2013).
22. N. A. Hosny et al., Direct imaging of changes in aerosol particle viscosity upon hydration and chemical aging. *Chem. Sci. (Camb.)* **7**, 1357–1367 (2016).
23. S. Gligorovski, J. P. D. Abbatt, An indoor chemical cocktail. *Science* **359**, 632–633 (2018).
24. H. Shen et al., Global atmospheric emissions of polycyclic aromatic hydrocarbons from 1960 to 2008 and future predictions. *Environ. Sci. Technol.* **47**, 6415–6424 (2013).
25. S. Zhou, L. W. Y. Yeung, M. W. Forbes, S. Mabury, J. P. D. Abbatt, Epoxide formation from heterogeneous oxidation of benzo[a]pyrene with gas-phase ozone and indoor air. *Environ. Sci. Process. Impacts* **19**, 1292–1299 (2017).
26. J. N. Pitts et al., Factors influencing the reactivity of polycyclic aromatic hydrocarbons adsorbed on filters and ambient POM with ozone. *Chemosphere* **15**, 675–685 (1986).
27. C. H. Wu, I. Salmeen, H. Niki, Fluorescence spectroscopic study of reactions between gaseous ozone and surface-adsorbed polycyclic aromatic hydrocarbons. *Environ. Sci. Technol.* **18**, 603–607 (1984).
28. L. Van Vaeck, K. Van Cauwenberghe, Conversion of polycyclic aromatic hydrocarbons on diesel particulate matter upon exposure to ppm levels of ozone. *Atmos. Environ.* **18**, 323–328 (1984).

29. D. A. Lane, M. Katz, The photomodification of benzo[a]pyrene, benzo[b]fluoranthene and benzo[k]fluoranthene under simulated atmospheric conditions. *Adv. Environ. Sci. Tech.* **8**, 137–154 (1977).

30. M. Shiraiwa, C. Pfrang, U. Pöschl, Kinetic multi-layer model of aerosol surface and bulk chemistry (KM-SUB): The influence of interfacial transport and bulk diffusion on the oxidation of oleic acid by ozone. *Atmos. Chem. Phys.* **10**, 3673–3691 (2010).

31. A. Zuend, C. Marcolli, B. P. Luo, T. Peter, A thermodynamic model of mixed organic-inorganic aerosols to predict activity coefficients. *Atmos. Chem. Phys.* **8**, 4559–4593 (2008).

32. A. Zuend et al., New and extended parameterization of the thermodynamic model AIOMFAC: Calculation of activity coefficients for organic-inorganic mixtures containing carboxyl, hydroxyl, carbonyl, ether, ester, alkenyl, alkyl, and aromatic functional groups. *Atmos. Chem. Phys.* **11**, 9155–9206 (2011).

33. A. Zuend, J. H. Seinfeld, A practical method for the calculation of liquid–liquid equilibria in multicomponent organic–water–electrolyte systems using physicochemical constraints. *Fluid Phase Equilib.* **337**, 201–213 (2013).

34. M. Shiraiwa et al., The role of long-lived reactive oxygen intermediates in the reaction of ozone with aerosol particles. *Nat. Chem.* **3**, 291–295 (2011).

35. L. Renbaum-Wolff et al., Viscosity of α-pinene secondary organic material and implications for particle growth and reactivity. *Proc. Natl. Acad. Sci. U.S.A.* **110**, 8014–8019 (2013).

36. A. Bjoerseth, T. Ramdahl, *Handbook of Polycyclic Aromatic Hydrocarbons, Volume 2, Emission Sources and Recent Progress in Analytical Chemistry* (Marcel Dekker, Inc., New York, NY, 1985).

37. A. C. Vander Wall et al., Understanding interactions of organic nitrates with the surface and bulk of organic films: Implications for particle growth in the atmosphere. *Environ. Sci. Process. Impacts* **20**, 1593–1610 (2018).

38. Y. J. Li et al., Chemical reactivity and liquid/nonliquid states of secondary organic material. *Environ. Sci. Technol.* **49**, 13264–13274 (2015).

39. D. M. Lienhard et al., Viscous organic aerosol particles in the upper troposphere: Diffusivity-controlled water uptake and ice nucleation? *Atmos. Chem. Phys.* **15**, 13599–13613 (2015).

40. O. Vesna, M. Sax, M. Kalberer, A. Gaschen, M. Ammann, Product study of oleic acid ozonolysis as function of humidity. *Atmos. Environ.* **43**, 3662–3669 (2009).

41. J. Zahardis, G. A. Petrucci, The oleic acid-ozone heterogeneous reaction system: Products, kinetics, secondary chemistry, and atmospheric implications of a model system–A review. *Atmos. Chem. Phys.* **7**, 1237–1274 (2007).

42. J. Zahardis, S. Geddes, G. A. Petrucci, The ozonolysis of primary aliphatic amines in fine particles. *Atmos. Chem. Phys.* **8**, 1181–1194 (2008).

43. D. G. Nash, M. P. Tolocka, T. Baer, The uptake of O_3 by myristic acid-oleic acid mixed particles: Evidence for solid surface layers. *Phys. Chem. Chem. Phys.* **8**, 4468–4475 (2006).

44. C. Pfrang, M. Shiraiwa, U. Pöschl, Chemical ageing and transformation of diffusivity in semi-solid multi-component organic aerosol particles. *Atmos. Chem. Phys.* **11**, 7343–7354 (2011).

45. R. M. Maertens et al., Mutagenic and carcinogenic hazards of settled house dust. I: Polycyclic aromatic hydrocarbon content and excess lifetime cancer risk from pre-school exposure. *Environ. Sci. Technol.* **42**, 1747–1753 (2008).

46. C. J. Weschler, N. Carslaw, Indoor chemistry. *Environ. Sci. Technol.* **52**, 2419–2428 (2018).

47. C. J. Weschler, W. W. Nazaroff, SVOC exposure indoors: Fresh look at dermal pathways. *Indoor Air* **22**, 356–377 (2012).

48. C. J. Weschler, W. W. Nazaroff, Growth of organic films on indoor surfaces. *Indoor Air* **27**, 1101–1112 (2017).

49. Q.-T. Liu, R. Chen, B. E. McCarry, M. L. Diamond, B. Bahavar, Characterization of polar organic compounds in the organic film on indoor and outdoor glass windows. *Environ. Sci. Technol.* **37**, 2340–2349 (2003).

50. C. J. Weschler, Ozone in indoor environments: Concentration and chemistry. *Indoor Air* **10**, 269–288 (2000).

51. S. Zhou, M. W. Forbes, J. P. D. Abbatt, Application of direct analysis in real time-mass spectrometry (DART-MS) to the study of gas-surface heterogeneous reactions: Focus on ozone and PAHs. *Anal. Chem.* **87**, 4733–4740 (2015).

52. Y. Cheng, H. Su, T. Koop, E. Mikhailov, U. Pöschl, Size dependence of phase transitions in aerosol nanoparticles. *Nat. Commun.* **6**, 5923 (2015).

53. G. Biskos, L. M. Russell, P. R. Buseck, S. T. Martin, Nanosize effect on the hygroscopic growth factor of aerosol particles. *Geophys. Res. Lett.* **33**, L07801 (2006).

54. M. B. Altaf, A. Zuend, M. A. Freedman, Role of nucleation mechanism on the size dependent morphology of organic aerosol. *Chem. Commun. (Camb.)* **52**, 9220–9223 (2016).

55. J. Ovadnevaite et al., Surface tension prevails over solute effect in organic-influenced cloud droplet activation. *Nature* **546**, 637–641 (2017).

EARTH, ATMOSPHERIC, AND PLANETARY SCIENCES